BULLETIN OF THE POLISH ACADEMY OF SCIENCES
TECHNICAL SCIENCES, Vol. 63, No. 3, 2015
DOI: 10.1515/bpasts-2015-0092

Modeling and control of a skid-steering mobile platform with coupled side wheels

K. TCHOŃ*, K. ZADARNOWSKA, Ł. JUSZKIEWICZ, and K. ARENT

Chair of Cybernetics and Robotics, Electronics Faculty, Wrocław University of Technology,
11/17 Janiszewskiego St., 50-372 Wrocław, Poland

Abstract. This study is devoted to the modeling and control of a 4-wheel, skid-steering mobile platform with coupled side wheels, subject to lateral and longitudinal slips. The dynamics equations of the platform are derived, and 16 variants of motion distinguished. For the variant of motion allowing for all possible slips of the wheels two control problems are addressed: the motion planning problem and the trajectory tracking problem. The former problem is solved by means of a Jacobian motion planning algorithm based on the Endogenous Configuration Space Approach and, complementarily, using the Optimal Control Approach. The Nonlinear Model Predictive Control is applied to the latter problem. Performance of these control algorithms is illustrated by a sort of the parking problem. Significant robustness of the predictive control algorithm against the model uncertainty is revealed.

Key words: wheeled mobile platform, dynamics, motion planning, trajectory tracking.

1. Introduction

An increase of robot autonomy belongs to the challenges of contemporary search and rescue robotics [1]. In response to this challenge the Polish National Centre for Research and Development has launched the project RobREx focused on improving autonomy of the rescue and exploration robots. The project's main research hypothesis is that the robot's autonomy can be achieved by equipping the robot with control algorithms based on the model of its dynamics. This objective is to be achieved by intertwined design and modeling phases in the robot development. As a consequence, the mobile platform Rex is being designed, presented in Fig. 1. The Rex platform is a 4-wheel, skid-steering platform, whose wheels can either be driven independently or coupled sidewise. The platform serves as a mobile basis of the mobile manipulator RobRex, intended for inspection tasks, both indoor as well as outdoor. The guidelines of design of the platform Rex have been sketched in [2]. The design of its control system is following the principles formulated in [3].

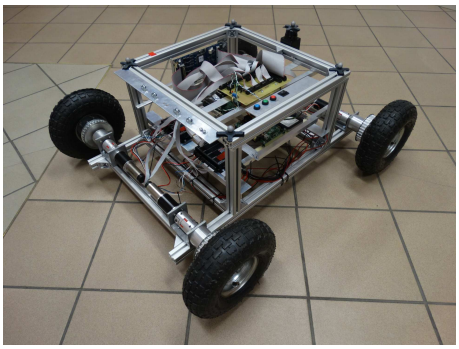

Fig. 1. Rex platform: actual view

This study addresses the problems of modeling and control of the mobile platform Rex based on the model of its dynamics. Throughout this study it has been assumed that the side wheels of the platform are coupled, the case of independently driven wheels is analyzed in [4]. A classical reference dealing with skid-steering mobile platforms is [5], that in the RobREx project has inspired a research direction explored in [6], whose methodology may be traced back to [7]. The approach presented here, motivated by nonholonomic robotics [8], the theory of automotive systems [9, 10], and the application of predictive control reported in [11], is based on more general assumptions, including lateral and longitudinal slips and an under actuated model of the platform dynamics. The dynamics equations of the Rex platform can be derived classically [12]. It is assumed that the wheels that are not permitted to slip are subject to traction forces, while the slips are counteracted by slip reaction forces. In the case of no slip, the traction forces are computed on the basis of the d'Alembert principle. A simple linear in the slip model of these forces has been employed, equivalent to the linearization of the model introduced in [13, 14]. All forces have been defined as the generalized forces, in the spirit of [15]. Friction in the drives and actuators is assumed known and compensated by feedback. Taking into account possible combinations of the slips, 16 variants of motion can be defined, starting from the motion completely without slips and ending with the motion admitting all kinds of slips. Each variant of motion is represented by a control affine system whose state space dimension varies from 6 up to 10. The dynamics model reflecting all the variants of motion results in a sort of switched system in which specific subsystems are switched on and off dynamically, depending on the road condition. A somewhat similar system is studied in [16], however in our case the switched subsystems

*e-mail: krzysztof.tchon@pwr.edu.pl

are control systems, and the switching is autonomous [17]. Alternatively, the totality of the platform motions could be regarded as a stratified system [18]. The control of the resulting switched system seems to be beyond the available analytic tools; on the other hand, it is rather unlikely to observe all 16 variants of motion during a mission of the Rex platform. For these reasons we have focused on two limit variants of motion: the motion without any slip and the motion with all slips permitted. The first case is easy, tantamount to a straight line motion with constant orientation. The second case, involving any curved motion, is analyzed in detail in the sequel.

Two control problems of the Rex platform moving with all possible slips is studied: the motion planning problem and the trajectory tracking problem. The motion planning problem consists in defining a control steering the platform to a desired position and orientation. This control produces a reference trajectory of motion of the platform. Given the reference trajectory, the trajectory tracking problem determines a control able to track the reference. The motion planning problem can be solved either by means of the Endogenous Configuration Space Approach (ECSA), [19,20] or the classical Optimal Control Approach (OCA). The trajectory tracking problem is solved using the Nonlinear Model Predictive Control (NMPC) method [21]. An advantage of the predictive control results from its robustness to the incomplete knowledge of the platform dynamics, particularly the traction/reaction and friction parameters. Both the OCA as well as NMPC are implemented with the use of the ACADO (Automatic Control and Dynamic Optimization) software package [22], dedicated to this type of problems. Performance of the proposed control algorithms is illustrated on a sort of parking problem. To reveal the robustness of the predictive control, the algorithm is applied in the case when the real platform parameters differ substantially from the nominal ones. Recently, a comprehensive overview of modeling and control issues of wheeled mobile robots has been presented in the monograph [23]. Due to their outstanding applied dimension, results of this monograph may appear of vital significance at the implementation stage of our approach.

This study is organized in the following way. Section 2 introduces a control theoretic model of the platform dynamics. Three variants of the platform motion are specified in Sec. 3. In Sec. 4 two control problems: the motion planning problem and the trajectory tracking problem are defined, along with suitable control algorithms. Section 5 gathers computational results. Section 6 contains conclusions.

2. Dynamics equations

The Rex platform has been intended to serve as a tool for implementing and testing model-based motion control algorithms. The platform's geometric schematic is displayed in Fig. 2. is a 4-wheel, skid-steering type mobile platform. Its wheels are identical, and can either be steered independently or coupled sidewise. In what follows it is assumed that the left and the right wheels of the platform have been coupled and are actuated by the same motor. The platform motion is described with respect to the global reference frame (X_0, Y_0, Z_0) with Z-axis pointing upward. The local frame (X, Y, Z) is placed in the middle of the platform rear axle, with Z-axis pointing upward and X-axis set along the platform, directed forward. Having defined the left and right wheel rotation angles $\theta_1 = \theta_2 = \theta_{12}$ and $\theta_3 = \theta_4 = \theta_{34}$, we obtain a vector of generalized coordinates of the platform $q = (x, y, \varphi, \theta_{12}, \theta_{34})^T \in \mathbb{R}^5$ consisting of the position of the middle point of the platform rear axle, the platform orientation, and the rotation angles of the wheels, cf. Fig. 2. In order to obtain the dimensional consistency of the coordinates, we represent the vector of generalized coordinates in the form $w = (x, y, a\varphi, R\theta_{12}, R\theta_{34})^T$, with R denoting the wheel radius, and a being the distance between the platform rear and front axes. It is easily seen that the Pfaffian matrix related to the lateral and longitudinal slips of the platform wheels takes the following form

$$H(w) = \begin{bmatrix} -\sin\frac{w_3}{a} & \cos\frac{w_3}{a} & 0 & 0 & 0 \\ -\sin\frac{w_3}{a} & \cos\frac{w_3}{a} & 1 & 0 & 0 \\ \cos\frac{w_3}{a} & \sin\frac{w_3}{a} & -\frac{b}{a} & -1 & 0 \\ \cos\frac{w_3}{a} & \sin\frac{w_3}{a} & \frac{b}{a} & 0 & -1 \end{bmatrix} = \begin{bmatrix} H^1(w) \\ H^2(w) \\ H^3(w) \\ H^4(w) \end{bmatrix}. \tag{1}$$

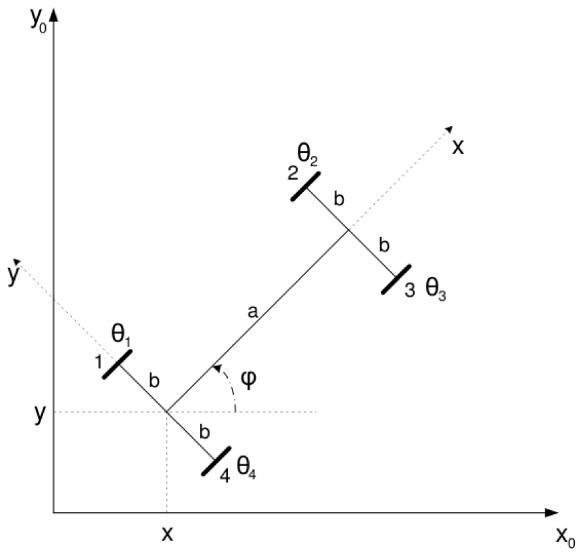

Fig. 2. Rex platform: geometric schematic

Subsequent rows of the matrix (1) define four possible slips of the platform wheels:

- the lateral slip of rear wheels $s_1 = H^1(w)\dot{w}$,
- the lateral slip of front wheels $s_2 = H^2(w)\dot{w}$,
- the longitudinal slip of left wheels $s_3 = H^3(w)\dot{w}$,
- the longitudinal slip of right wheels $s_4 = H^4(w)\dot{w}$.

Consequently, the identity of the form

$$H^i(w)\dot{w} = 0, \quad i = 1, 2, 3, 4,$$

describes the motion of the platform without a corresponding slip. By assuming that this identity holds for 4, 3, 2, 1 or 0 rows out of the four of the Pfaffian matrix (1), we arrive at

$$\binom{4}{4}+\binom{4}{3}+\binom{4}{2}+\binom{4}{1}+\binom{4}{0}=2^4=16$$

admissible variants of motion of the Rex platform. In particular, the condition $H(w)\dot{w}=0$ refers to the totally slip-less motion, whereas $0\dot{w}=0$ means allowing for all possible slips.

For a further reference we shall encode every variant of motion by a 4-digit binary number $\alpha=\alpha_1\alpha_2\alpha_3\alpha_4$, $\alpha_i=0,1$, in such a way that $\alpha_i=1$ means that the i-th motion constraint $H^i(w)\dot{w}=0$ is enabled, while $\alpha_i=0$ disables this constraint. Each number α determines a sub-matrix $H^\alpha(w)$ of the Pfaffian matrix, consisting of rows corresponding to the positions of non-zero digits in α. Specifically, if $\alpha=0101$ then

$$H^\alpha(w)=\begin{bmatrix}H^2(w)\\H^4(w)\end{bmatrix},$$

so $H^\alpha(w)\dot{w}=0$ means the motion without the lateral slip of the front wheels and without the longitudinal slip of the right wheels of the platform.

Assuming that the platform Rex moves on the horizontal plane, and that the wheels touch the ground point-wise, its dynamics can be represented by the following control system

$$P(w)\ddot{w}+D(w,\dot{w})=F(w,\dot{w})+B(w)u,\quad \mathrm{y}=k(w). \quad (2)$$

In the above equations $P(w)$ denotes the inertia matrix, $D(w,\dot{w})$ refers to centripetal and Coriolis forces, $F(w,\dot{w})=F_f(w,\dot{w})+F_t(w,\dot{w})+F_s(w,\dot{w})$ describes friction, traction and slip reaction forces at the contact points of the wheels with the ground, $B(w)=\frac{1}{R}\left[0_{2\times3},\ \mathbb{I}_2\right]^T$ is the control matrix. The control inputs $u=(u_1,u_2)^T\in\mathbb{R}^2$ have the sense of torques exerted by the motors on the coupled left and right wheels. The output function $k(w)=(w_1,w_2,\frac{w_3}{a})^T$ provides the platform's position and orientation. The following form of $P(w)$ and $D(w,\dot{w})$ has been found

$$P(w)=\begin{bmatrix}Q_{11} & 0 & \frac{Q_{13}}{a} & 0 & 0\\ 0 & Q_{22} & \frac{Q_{23}}{a} & 0 & 0\\ \frac{Q_{13}}{a} & \frac{Q_{23}}{a} & \frac{Q_{33}}{a^2} & 0 & 0\\ 0 & 0 & 0 & \frac{Q_{44}}{R^2} & 0\\ 0 & 0 & 0 & 0 & \frac{Q_{55}}{R^2}\end{bmatrix}, \quad (3)$$

$$D(w,\dot{w})=\frac{\dot{w}_3^2}{a^2}\begin{pmatrix}-Q_{23}\\ Q_{13}\\ 0\\ 0\\ 0\end{pmatrix},$$

where

$$Q_{11}=Q_{22}=m_p+4m_w,\quad Q_{44}=Q_{55}=2I_{w33},$$

$$Q_{13}=-m_p\left(a_{p1}\sin\frac{w_3}{a}+a_{p2}\cos\frac{w_3}{a}\right)-2m_wa\sin\frac{w_3}{a},$$

$$Q_{23}=m_p\left(a_{p1}\cos\frac{w_3}{a}-a_{p2}\sin\frac{w_3}{a}\right)+2m_wa\cos\frac{w_3}{a},$$

$$Q_{33}=I_{p33}+m_p(a_{p1}^2+a_{p2}^2)+4(I_{w11}+m_wb^2)+2m_wa^2.$$

The symbols used above have the following meaning: m_p, m_w – mass of the platform and of a single wheel, a_{p1} and a_{p2} – position of the platform mass center in the local frame, I_{w11}, I_{w33} – wheel's moments of inertia with respect to Y and Z axis of the local frame, I_{p33} – the platform moment of inertia with respect to Z axis of the local frame, a, b - the length and the width of the platform, R – the radius of each wheel.

The generalized forces standing on the right hand side of the dynamics Eq. (2), beyond controls, contain the generalized friction, traction and slip reaction forces. The friction forces describe the transmission of actuating torques from the motors to the wheels as well as all the other kinds of friction. In the simplest case it may be assumed that

$$F_f(w,\dot{w})=(0,0,0-\gamma_1\dot{w}_4,-\gamma_2\dot{w}_5)^T,$$

where $\gamma_i>0$ denote the viscous friction coefficients. Acting solely on the actuated generalized coordinates, the friction forces can be compensated by a feedback, so in what follows they are omitted. Concerning the traction and reaction forces, suppose that the Pfaffian motion constraints imposed on the platform have the form $H^\alpha(w)\dot{w}=0$, for a certain α. Then, according to the d'Alembert principle, the generalized traction forces take the form

$$F_t(w,\dot{w})=H^{\alpha\,T}(w)\lambda_\alpha,$$

λ_α denoting a Lagrange multiplier. As far as $\alpha\neq1111$, some slips of the wheels appear. Assume temporarily that not all slips are allowed, so also $\alpha\neq0000$. Let $s_j=H^j(w)\dot{w}$ denote an admissible slip. It is assumed that the presence of this slip induces at the contact point of the wheel with the ground a reaction force $r_j=-\beta_js_j=-\beta_jH^j(w)\dot{w}$ proportional to the slip and counteracting the slip. Since the slips have the sense of velocities, this means that the slip reaction acts like a linear dumper. The slip reaction coefficients β_j depend on the normal force N_i exerted by the wheel i on the ground, and on the properties of the ground at the contact point, specifically, $\beta_1=\varepsilon_1N_1+\varepsilon_4N_4$, $\beta_2=\varepsilon_2N_2+\varepsilon_3N_3$, $\beta_3=\tau_1N_1+\tau_2N_2$, and $\beta_4=\tau_3N_3+\tau_4N_4$, where ε_i, τ_i refer, respectively, to the lateral and the longitudinal slip of the wheel i. Given the force r_j, the corresponding generalized slip reaction force $F_{s\,j}(w,\dot{w})$ can be found using the virtual work principle. Supposing that $r_js_j=r_jH^j(w)\dot{w}=F_{s\,j}^T(w,\dot{w})\dot{w}$, we conclude that $F_{s\,j}(w,\dot{w})=H^{j\,T}(w)r_j$. Given $\alpha=\alpha_1\alpha_2\alpha_3\alpha_4$, we define $\overline{\alpha}=\overline{\alpha}_1\overline{\alpha}_2\overline{\alpha}_3\overline{\alpha}_4$, where $\overline{\alpha}_i$ is the negation of α_i. It is easily checked that, if the traction forces $F_t(w,\dot{w})=H^{\alpha\,T}(w)\lambda_\alpha$ then the generalized slip reaction forces can be written down as

$$F_s(w,\dot{w})=H^{\overline{\alpha}\,T}(w)r_{\overline{\alpha}},$$

for

$$r_{\overline{\alpha}}=-diag\{\beta_{\overline{\alpha}}\}H^{\overline{\alpha}}(w)\dot{w},$$

where $diag\{\beta_{\overline{\alpha}}\}$ is a diagonal matrix. Summarizing the above assumptions, for a given variant of motion α, the dynamics

equations of the Rex platform can be represented in the following form

$$\begin{cases} P(w)\ddot{w}+D(w,\dot{w})=H^{\alpha\,T}(w)\lambda_\alpha+H^{\overline{\alpha}\,T}(w)r_{\overline{\alpha}}+B(w)u, \\ \mathrm{y}=k(w). \end{cases} \tag{4}$$

The Pfaffian constraints $H^\alpha(w)\dot{w}=0$ represent the platform kinematics in the α variant of motion, and are tantamount to a driftless control system

$$\dot{w}=G^\alpha(w)\eta_\alpha,$$

where $G^\alpha(w)$ is a matrix whose columns span the null space of $H^\alpha(w)$, and η_α has a suitable dimension. Since $H^\alpha(w)G^\alpha(w)=0$, it follows that by multiplying the dynamics Eqs. (4) from the left by $G^{\alpha\,T}(w)$ we can eliminate the traction forces. Furthermore, after a substitution of $\ddot{w}$ in (4) by $\dot{G}^\alpha(w)\eta_\alpha+G^\alpha(w)\dot{\eta}_\alpha$, we obtain the following motion equations in the α variant of motion

$$\begin{cases} \dot{w}=G^\alpha(w)\eta_\alpha \\ \dot{\eta}_\alpha=\left(G^{\alpha\,T}(w)P(w)G^\alpha(w)\right)^{-1}G^{\alpha\,T}(w) \\ \left(P(w)\dot{G}^\alpha(w)\eta_\alpha-D(w,\dot{w})+H^{\overline{\alpha}\,T}(w)r_{\overline{\alpha}}+B(w)u\right), \\ \mathrm{y}=k(w), \quad r_{\overline{\alpha}}=-diag\{\beta_{\overline{\alpha}}\}H^{\overline{\alpha}}(w)\dot{w}. \end{cases} \tag{5}$$

Having solved these equations for w, the traction forces are computed from (4) as

$$F_t(w,\dot{w})=P(w)\ddot{w}+D(w,\dot{w})-H^{\overline{\alpha}\,T}(w)r_{\overline{\alpha}}-B(w)u. \tag{6}$$

3. Specification

In this section we shall specify the motion Eqs. (5) of the Rex platform to three example variants of motion.

3.1. No slip permitted, $\alpha=1111$. In this case the platform motion satisfies full Pfaffian constraints (1), so $H^\alpha(w)=H(w)$, whereas $H^{\overline{\alpha}}(w)=0$, so the slip reaction forces are absent. Since $G^\alpha(w)=\left(\cos\frac{w_3}{a},\sin\frac{w_3}{a},0,1,1\right)^T$, then $\eta_\alpha\in\mathbb{R}$, and the kinematics part of (5) takes the form

$$\dot{w}=\left(\cos\frac{w_3}{a},\sin\frac{w_3}{a},0,1,1\right)^T\eta_\alpha.$$

In particular, this implies that $\dot{w}_3=0$, i.e. the platform moves along a straight line, with a fixed orientation. Consequently, we get $D(w,\dot{w})=0$, $\dot{G}^\alpha(w)=0$, and conclude that the dynamics part of the platform motion is governed by a single equation

$$\dot{\eta}_\alpha=\frac{1}{Q_{11}R+\dfrac{2Q_{44}}{R}}(u_1+u_2).$$

As can be seen, altogether the platform motion is determined by 6 differential equations. The traction forces are defined by suitably modified (6). It follows that the traction forces act at the contact points of wheels with the ground, in the direction parallel or perpendicular to the the wheel axle. Therefore, as long as these forces are less than the static friction forces at the contact points, the platform motion remains within the variant $\alpha=1111$. Increasing the control torques results in the situation when the friction is no longer able to provide sufficient traction, so the variant of platform motion changes, e.g. both the rear and the front wheels start to slip laterally, $\alpha=0011$. By design, forcing a lateral slip is necessary to change the orientation of the Rex platform. This case is studied in more detail in the next subsection.

3.2. Lateral slips permitted, $\alpha=0011$. We have the motion without longitudinal slips, so the motion constraints become $H^\alpha(w)\dot{w}=0$, where

$$H^\alpha(w)=\begin{bmatrix}\cos\frac{w_3}{a} & \sin\frac{w_3}{a} & -\frac{b}{a} & -1 & 0\\ \cos\frac{w_3}{a} & \sin\frac{w_3}{a} & \frac{b}{a} & 0 & -1\end{bmatrix}.$$

Consequently, we have

$$H^{\overline{\alpha}}(w)=\begin{bmatrix}-\sin\frac{w_3}{a} & \cos\frac{w_3}{a} & 0 & 0 & 0\\ -\sin\frac{w_3}{a} & \cos\frac{w_3}{a} & 1 & 0 & 0\end{bmatrix}.$$

Having computed

$$G^\alpha(w)=\begin{bmatrix}\cos\frac{w_3}{a} & \sin\frac{w_3}{a} & 0 & 1 & 1\\ 0 & 0 & 1 & -\frac{b}{a} & \frac{b}{a}\\ \sin\frac{w_3}{a} & -\cos\frac{w_3}{a} & 0 & 0 & 0\end{bmatrix}^T,$$

we obtain the motion equations of the platform in the form

$$\begin{cases} \dot{w}=G^\alpha(w)\eta_\alpha \\ \dot{\eta}_\alpha=\left(G^{\alpha\,T}(w)P(w)G^\alpha(w)\right)^{-1}G^{\alpha\,T}(w) \\ \left(P(w)\dot{G}^\alpha(w)\eta_\alpha-D(w,\dot{w})+H^{\overline{\alpha}\,T}(w)r_{\overline{\alpha}}+B(w)u\right), \\ \mathrm{y}=k(w), \end{cases}$$

where $\eta_\alpha\in\mathbb{R}^3$, and $r_{\overline{\alpha}}=-\beta_{\overline{\alpha}}H^{\overline{\alpha}}(w)\dot{w}$, for $\beta_{\overline{\alpha}}=diag\{\beta_1,\,\beta_2\}$.

The system of equations of motion is 8-dimensional. If, additionally, the traction forces necessary to prevent longitudinal slips are bigger than the corresponding friction forces at the contact points of the wheels with the ground, the platform passes to the variant of motion with all slips permitted, characterized by $\alpha=0000$.

3.3. All slips permitted, $\alpha=0000$. In this type of motion, there act only the slip reaction forces at the contacts of wheels with the ground. We have $H^\alpha(w)=0$, therefore $G^\alpha(w)=\mathbb{I}_5$. Also, $H^{\overline{\alpha}}(w)=H(w)$, $\eta_\alpha\in\mathbb{R}^5$, $\lambda_\alpha=0$, so the motion equations take the form

$$\begin{cases} \dot{w}=\eta_\alpha \\ P(w)\dot{\eta}_\alpha+D(w,\dot{w})=-H^T(w)\beta H(w)\dot{w}+B(w)u, \\ \mathrm{y}=k(w), \end{cases}$$

where the diagonal matrix $\beta=diag\{\beta_i\}$ collects all the slip reaction coefficients considered in Sec. 2. The motion equations are 10-dimensional. Observe that the control torques are

transmitted to the position and orientation coordinates only through the slip reactions.

4. Control

It has been shown in Sec. 2 that the platform motion can be described by a collection of 16 systems of equations of the form (5) involving two control inputs, each labelled by an α, switched on and off in time. Either the number of variables appearing in these equations, varying from 6 to 10, or the switching times are not known a priori, but depend on the history of motion/actuation. The presence of autonomous switching in the motion equations makes the control and motion planning of the Rex platform extremely hard. On the other hand, it may be expected that not all variants of motion are equally meaningful from a practical point of view. Specifically, it seems that two limit variants are most significant, namely those described by $\alpha = 1111$ and $\alpha = 0000$. As has been shown in the previous section, the former case is easy, tantamount to controlling a simple linear control system. For this reason, below we shall focus on the latter case, whose motion equations are represented by a control affine system with output function. Specifically, the motion Eqs. (2) yield

$$\dot{x} = f(x) + g(x)u = f(x) + \sum_{i=1}^{m} g_i(x)u_i, \quad y = k(x), \quad (7)$$

where

$$x = (w, \dot{w}) = (x^1, x^2) \in \mathbb{R}^{10},$$

$$g(x) = \left[0_{5\times 2},\, P^{-1}(x^1)B\right],$$

and

$$u \in \mathbb{R}^2, \quad f(x) = \left(x^2, P^{-1}(x^1)(-D(x) + F(x))\right).$$

By definition, all vector fields and functions appearing in (7) are smooth. Let $T > 0$ denote a control time horizon. Suppose that admissible control functions belong to the Hilbert space $L^2_m[0,T]$ equipped with the inner product $\langle u_1(\cdot), u_2(\cdot)\rangle = \int_0^T u_1^T(t)u_2(t)dt$. The space of control functions $\mathcal{X} = L^2_m[0,T]$ is referred to as the endogenous configuration space. Let for the given control $u(\cdot)$, $x(t) = \varphi_{x_0,t}(u(\cdot))$ be the state trajectory of the control system initialized at x_0. The corresponding output trajectory $y(t) = k(x(t))$. Then, the end point map of the system (7)

$$K_{x_0,T}(u(\cdot)) = k(x(T)) = k(\varphi_{x_0,T}(u(\cdot))) \quad (8)$$

determines the system output response at T to the control function $u(\cdot)$.

4.1. Motion planning. Given the system (7), we shall study the following motion planning problem for the mobile platform subject to slipping: given a desired point y_d in the task space, the initial state x_0 and a time horizon T, find a control function $u_d(t)$, such that the system output, starting from an initial point $y_0 = k(x_0)$, reaches the desired point $K_{x_0,T}(u_d(\cdot)) = y_d$.

Endogenous Configuration Space Approach. The motion planning problem can be solved by a Jacobian motion planning algorithm derived within the Endogenous Configuration Space Approach (ECSA), [19]. This derivation can be summarized as follows. We start from an arbitrarily chosen initial control function $u_0(\cdot) \in \mathcal{X}$. If this function solves the problem, we are done. Otherwise, (i.e. when $K_{x_0,T}(u_0(\cdot)) \neq y_d$) we look for a differentiable curve $u_\theta(\cdot), \theta \in \mathbb{R}$ in $\mathcal{X}$, passing through $u_0(\cdot)$, such that the task space error $e(\theta) = K_{x_0,T}(u_\theta(\cdot)) - y_d$ along this curve decreases exponentially along with θ, with a prescribed rate of error decay $\gamma > 0$, i.e. $\frac{de(\theta)}{d\theta} = -\gamma e(\theta)$. After differentiating the error with respect to θ, we arrive at the identity

$$D\,K_{x_0,T}(u_\theta(\cdot))\frac{du_\theta(\cdot)}{d\theta} = J_{x_0,T}(u_\theta(\cdot))\frac{du_\theta(\cdot)}{d\theta} = -\gamma e(\theta), \quad (9)$$

where $v(\cdot) \in \mathcal{X}$. The operator

$$J_{x_0,T}(u(\cdot))v(\cdot) = \rho(T) = C(T)\int_0^T \Phi(T,s)B(s)v(s)ds \quad (10)$$

is called the Jacobian of the system (7) at the endogenous configuration $u(\cdot)$. For a given $v(\cdot)$, the Jacobian (10) determines the value at time T of the output $\rho(t)$ of the linear approximation

$$\dot{\xi}(t) = A(t)\xi(t) + B(t)v(t), \quad \rho(t) = C(t)\xi(t), \quad \xi(0) = 0, \quad (11)$$

to the system (7) along the control-trajectory pair $(u(t), x(t))$. This implies that the system matrices need to be computed as

$$A(t) = \frac{\partial(f(x(t)) + g(x(t))u(t))}{\partial x},$$

$$B(t) = g(x(t)), \qquad C(t) = \frac{\partial k(x(t))}{\partial x},$$

while the transition matrix $\Phi(t,s)$ is a solution of the differential equation

$$\frac{\partial \Phi(t,s)}{\partial t} = A(t)\Phi(t,s)$$

passing through $\Phi(s,s) = \mathbb{I}_{10}$. By plugging into (9) a right inverse $J^{\#}_{x_0,T}(u(\cdot))$ of the Jacobian (10), we obtain a Jacobian motion planning algorithm that provides a solution to the motion planning problem as the limit $u_d(t) = \lim_{\theta\to+\infty} u_\theta(t)$ of the solution of the functional differential equation

$$\frac{du_\theta(\cdot)}{d\theta} = -\gamma J^{\#}_{x_0,T}(u_\theta(\cdot))(K_{x_0,T}(u_\theta(\cdot)) - y_d), \quad (12)$$

initialized at $u_{\theta=0}(t) = u_0(t)$. Customarily, the Moore-Penrose Jacobian inverse is used that gives the Eq. (12) the form

$$\frac{du_\theta(t)}{d\theta} = -\gamma B^T_\theta(t)\Phi^T_\theta(T,t)C^T_\theta(T)\mathcal{G}^{-1}_{x_0,T}(u_\theta(\cdot)) \cdot (K_{x_0,T}(u_\theta(\cdot)) - y_d), \quad (13)$$

where the subscript θ means that the corresponding object needs to be computed along the control-trajectory pair $(u_\theta(t), x_\theta(t))$. The matrix $\mathcal{G}_{x_0,T}(u(\cdot))$ standing in (13) is the output Gram matrix of the linear approximation (11), referred

to as the mobility matrix of the system (7), [24]. This matrix can be computed by integrating the Lyapunov differential equation

$$\dot{M}(t) = B(t)B^T(t) + A(t)M(t) + M(t)A^T(t), \qquad (14)$$

with $M(0) = 0$, and setting $\mathcal{G}_{x_0,T}(u(\cdot)) = C(T)M(T)C^T(T)$. The Moore-Penrose Jacobian algorithm works outside singular endogenous configurations at which the mobility matrix gets singular. The presented Jacobian motion planning algorithm refers to the unconstrained problem. To deal with a motion problem with constraints this algorithm may be extended to either the imbalanced Jacobian [25] or the prioritized Jacobian algorithm [20].

The functional differential Eq. (13) can be solved using a finite trigonometric (Fourier) parametrization of the control functions, i.e. by setting $u_\lambda(t) = P_s(t)\lambda$, with $P_s(t) = diag\{P(t), P(t)\}$ denoting a block diagonal matrix built of 2 copies of the row matrix $P(t) = [1, \sin\omega t, \cos\omega t, \ldots, \cos p\omega t]$, $\omega = 2\pi/T$, containing $2p+1$ basic functions, $s = 2(2p+1)$. The vector $\lambda \in \mathbb{R}^s$ contains control parameters. The dimension s of the control space should be at least equal to the number of output coordinates in (7). After the parametrization of control functions, the Jacobian operator (10) converts to the matrix

$$J_{x_0,T}(\lambda) = C_\lambda(T) \int_0^T \Phi_\lambda(T,t)B_\lambda(t)P_s(t)dt \qquad (15)$$

defined along the control-trajectory pair $(u_\lambda(t), x_\lambda(t))$. It is easily seen that the parametric Jacobian $J_{x_0,T}(\lambda) = C_\lambda(T)J_\lambda(T)$, where $J_\lambda(t)$ solves the differential equation

$$\dot{J}_\lambda(t) = A_\lambda(t)J_\lambda(t) + B_\lambda(t)P_s(t), \qquad (16)$$

with initial condition $J_\lambda(0) = 0$. In the parametric setting and after applying the Euler scheme of integration, the Jacobian algorithm (13) gets equivalent to the updating of the control parameters

$$\lambda_{\theta+1} = \lambda_\theta - \gamma J^T_{x_0,T}(\lambda_\theta)\mathcal{G}^{-1}_{x_0,T}(\lambda_\theta)(K_{x_0,T}(\lambda_\theta) - y_d), \quad \theta = 0, 1, \ldots, \qquad (17)$$

starting from a certain λ_0, where the parametric mobility matrix $\mathcal{G}_{x_0,T}(\lambda) = J_{x_0,T}(\lambda)J^T_{x_0,T}(\lambda)$. The solution of the motion planning problem in the parametric setting is given as $u_d(t) = P_s(t)\lambda_d$, where $\lambda_d = \lim_{\theta\to+\infty}\lambda_\theta$.

Optimal Control Approach. Alternatively, a motion planning algorithm can be designed on the basis of the Optimal Control Approach (OCA). To this aim, the motion planning problem for system (7) is formulated as an optimal control problem with quadratic objective function

$$J_p(u(\cdot), x_0) = \int_0^T \big((y(t) - y_d)^T\mathcal{P}_p(y(t) - y_d) + u(t)^T\mathcal{R}_p u(t)\big)\, dt, \qquad (18)$$

involving symmetric matrices $\mathcal{P}_p \geq 0$ and $\mathcal{R}_p > 0$. Additionally, some constraints can be imposed, in the form $s(x(t), u(t)) \leq 0$ or $r(x(0), x(T)) \leq 0$, where the first inequality refers to the system's state trajectory and control, and the second sets up the accuracy of reaching the desired output. Numerical solution of the motion planning problem within OCA can be obtained by means of the methods of sequential quadratic programming and direct multiple shooting implemented in the ACADO software package [26]. The computations result in a control function $u_d(t)$ that solves the motion planning problem with prescribed accuracy. A substitution of this control to the system (7) allows to find a corresponding state trajectory $x_d(t)$ and an output trajectory $y_d(t)$. The latter serves as the reference trajectory in the trajectory tracking problem.

4.2. Tracking. Because the motion of the Rex platform takes place on a finite time interval, the trajectory tracking problem is defined in the following way: For a given reference output trajectory $y_d(t)$ of the system (7), find a control $u(t)$, such that the corresponding trajectory $y(t)$ stays close to the reference in a certain measurable sense. Specifically, the tracking problem can be formulated as the optimal control problem, with objective function

$$J_s(u(\cdot), x_0) = \int_0^T \big((y(t) - y_d(t))^T\mathcal{P}_s(y(t) - y_d(t)) + u(t)^T\mathcal{R}_s u(t)\big)\, dt, \qquad (19)$$

containing symmetric matrices $\mathcal{P}_s \geq 0$, $\mathcal{R}_s > 0$, and possibly including additional constraints imposed on the control functions. The control computed as a solution of the optimal control problem is by definition an open loop control, unable to cope with ubiquitous in practical situations modeling errors and measuring disturbances. A control strategy that joins the optimal control and the feedback control is the predictive control. Suppose that we have a real system and its model that takes the form of the nominal system (7). Due to modeling and measuring errors the optimal control computed for the nominal system may not guarantee the tracking in the real system. The Nonlinear Model Predictive Control (NMPC) consist in repeatedly solving the optimal control problem (19) in the system (7), over a time horizon $t_{pred} \leq T$ called the prediction time, and then applying this optimal control to the real system over the control time $t_{contr} \leq t_{pred}$, then computing the system current state/output, and finally resuming the optimal control problem (19) in the nominal system initialized by the the actual state/output of the real system. In this way the nominal model is used only over the control time, while the resulting control is updated systematically by the state of the real system in a way characteristic to the feedback control. For computational reasons the prediction time is divided into a number of subintervals on which the control is assumed constant, and the control time is taken as one of these intervals. Obviously, for $t_{contr} = t_{pred} = T$ the predictive control gets equivalent merely to the optimal control with the objective function (19). Similarly as in Subsec. (OCA), the NMPC solution of the trajectory tracking problem can be obtained by employing the ACADO package.

5. Simulation results

In this section we shall solve a motion planning problem and a trajectory tracking problem for the Rex platform, using the methods outlined in the previous section. The platform motion variant is $\alpha = 0000$, so that the system (7) is defined by the platform dynamics equations derived in Subsec. 3.3. A computation supported by the Autodesk Inventor 3D CAD software package provided the following values of the Rex platform parameters [27]: $m_p = 21.107$ kg, $m_w = 2.380$ kg, $a_{p1} = 0.377$ m, $a_{p2} = 0.008$ m, $a = 0.730$ m, $b = 0.350$ m, $R = 0.127$ m, $I_{p33} = 1.991$ kgm^2, $I_{w11} = 0.015$ kgm^2, $I_{w33} = 0.009$ kgm^2. The slip reaction force coefficients are set to $\epsilon_i = 1$, $\tau_i = 1.3$, $i = 1, 2, 3, 4$, and the normal forces exerted by each wheel are assumed the same.

5.1. Planning. The following motion planning problem is examined: Given the initial state $x_0 = (0, 0, a\frac{\pi}{2}, 0_{1\times 7})^T$, and the time horizon $T = 8$, find a control $u_d(t) \in \mathbb{R}^2$ driving the platform to the desired point $y_d = (10, 0, a\frac{\pi}{2})^T$. This problem is a sort of the parking manoeuvre.

ECSA. Firstly, the motion planning is solved by means of the algorithm (17). The controls are chosen in the form of truncated trigonometric series containing the constant and up to the 3rd order harmonics. The vector of initial values of the control parameters $\lambda_{0i} = (0.5, 0.01, 0.01, 0.001, 0.001, 0.0001, 0.0001)^T$, $i = 1, 2$. The error decay rate is set to $\gamma = 1$, and the computations are terminated when the error norm $||y(T) - y_d|| \leq 10^{-4}$. The computation results are shown in Fig. 3. They present the plat-

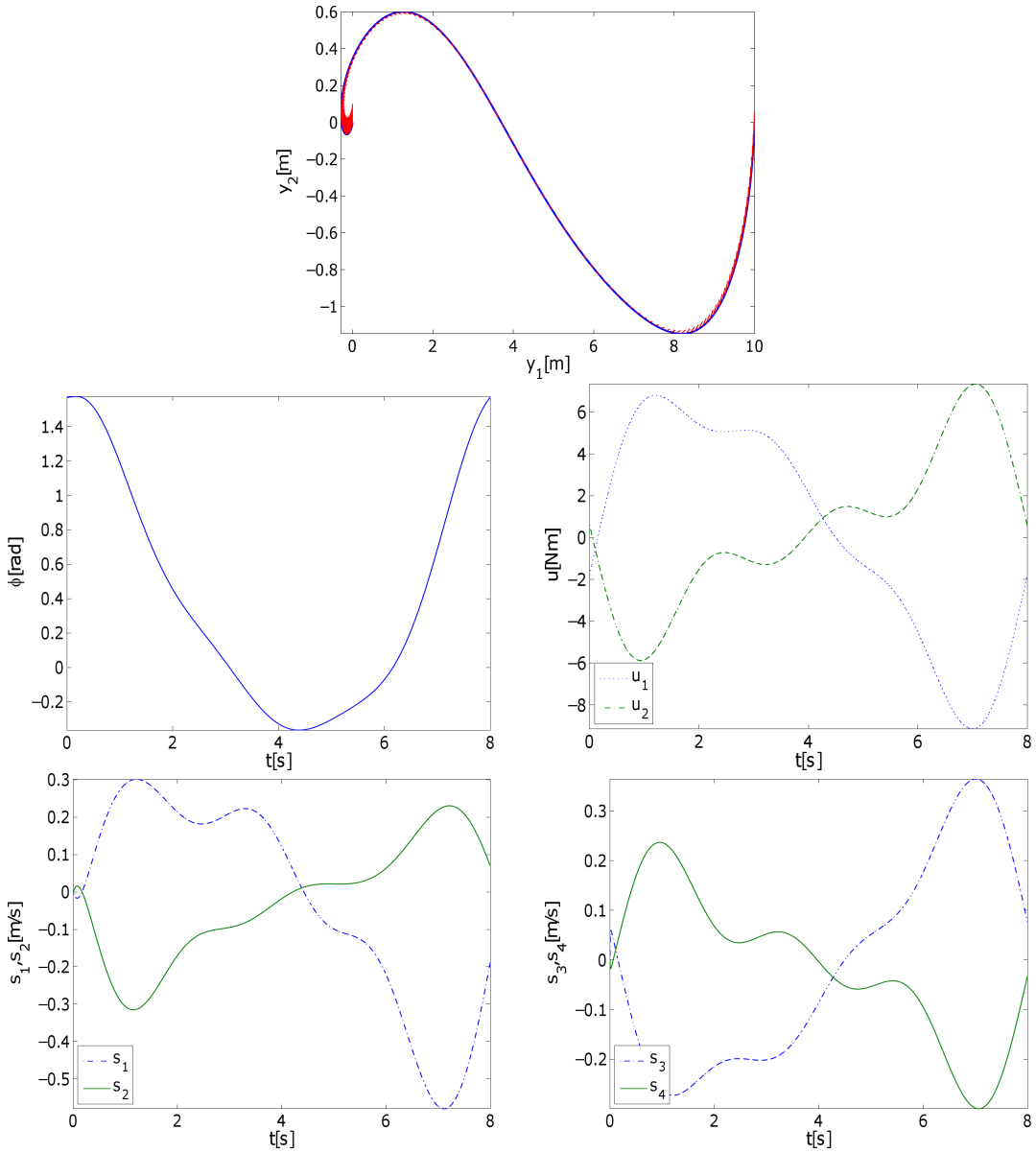

Fig. 3. Motion planning, ECSA: platform path, orientation, controls, lateral slips, longitudinal slips

form path, its orientation, controls, and slips. In order to visualize the effect of wheel slips, the platform orientation has been marked along the motion path. In the figure the original coordinates q are used instead of w, and the slips renamed as $s_1 = s_{14}$, $s_2 = s_{23}$, $s_3 = s_{12}$, $s_4 = s_{34}$. Observe that the slips at T do not vanish, since the platform has not been requested to stop at the destination point.

OCA. Next, the same motion planning problem is solved using OCA. In the objective function (18) the unit matrices $\mathcal{P}_p = \mathbb{I}_3$ and $\mathcal{R}_p = \mathbb{I}_4$ have been chosen, and constraints on the platform linear velocity and control torques imposed in the form

$$\sqrt{\dot{w}_1^2(t) + \dot{w}_2^2(t)} \leq 1.5 \text{ m/s} \quad \text{and} \quad |u_1(t)|, |u_2(t)| \leq 16 \text{ Nm}.$$

The accuracy of reaching the desired point is $|y_1(T) - y_{d1}|, |y_2(T) - y_{d2}| \leq 0.01$, $|y_3(T) - y_{d3}| \leq 0.05$. The resulting platform path and controls are displayed in Fig. 4.

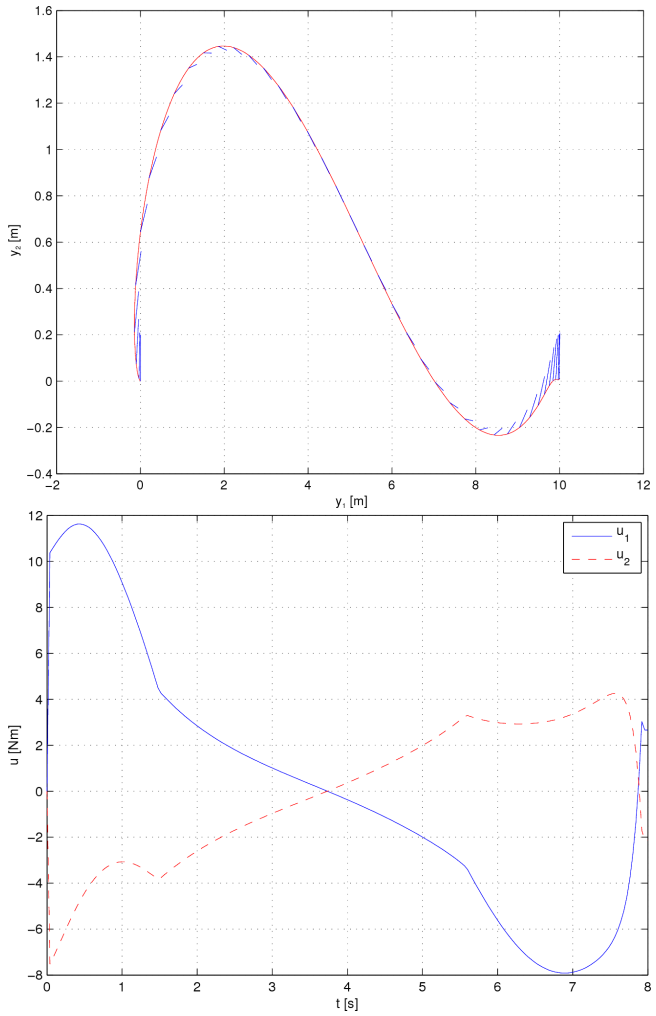

Fig. 4. Motion planning, OCA: platform path, controls

5.2. Tracking. The reference trajectory $y_d(t)$ has been taken as computed in Subsec. (OCA). The NMPC algorithm is employed, described in Subsec. 4.2, with the prediction time $t_{pred} = 1$ s, and the control time $t_{cont} = 25$ ms. In the objective function (19) we set $\mathcal{P}_s = diag\{100, 100, 10\}$ and $\mathcal{R}_s = 0.001\mathbb{I}_4$. The control bounds are $|u_i(t)| \leq 16$ Nm, $i = 1, 2$. The result of tracking $y_d(t)$ is presented in Fig. 5. This solution corresponds to the nominal parameters of Rex. For the purpose of demonstration of the robustness of predictive control against modeling errors, the predictive control algorithm has been applied in order to track the trajectory $y_d(t)$ in three perturbed systems. One of them has zero off diagonal elements of the inertia matrix (3) (so the term $D(w, \dot{w})$ vanishes), in two other the slip reaction force coefficients are deviated by ± 50 percent of their nominal values, at the nominal inertia matrix. In all the computations the platform starts from a point at the desired trajectory. Results are shown in Figs. 6–8. Despite considerable model deficiencies, the NMPC tracking turns out to be satisfactory.

5.3. Efficiency of computations. The computations have been run on a PC with Intel Core i5 2.30GHz processor. The solution of the motion planning problem using ECSA shown in Fig. 3 ($\gamma = 1$) was found in 44s. Using OCA and the ACADO simulation environment, the motion planning problem was solved in 83 s. Observe that the solutions provided by ECSA and OCA are completely different. These computation times, however, are not very critical as the motion planning problem need not be solved on line. The computation times of the solution of trajectory tracking problems varied between 282 s and 743 s, depending on the problem. This might suggest that presented algorithms and their ACADO implementation are not suitable for real time control of the Rex platform. However, it should be noticed that for the generic implementation of the optimal control in ACADO these times include not only the integration time of the model of the control system residing inside the controller, but also the simulation time of the controlled object. This situation may be alleviated by using the ACADO Code Generation tool, able to automatically generate an optimized and highly efficient C code dedicated to a specific NMPC controller. In our computations it was assumed that the control time $t_{contr} = 25$ ms, so for a real time control new values of controls need to be computed every 25 ms. The controller based on the generated C code needs approximately 12 ms to do this, making the NMPC real time control of the Rex platform entirely possible. Similarly, the code generation can speed up solving the motion planning problem, and reduce the computation time to approximately 2 s.

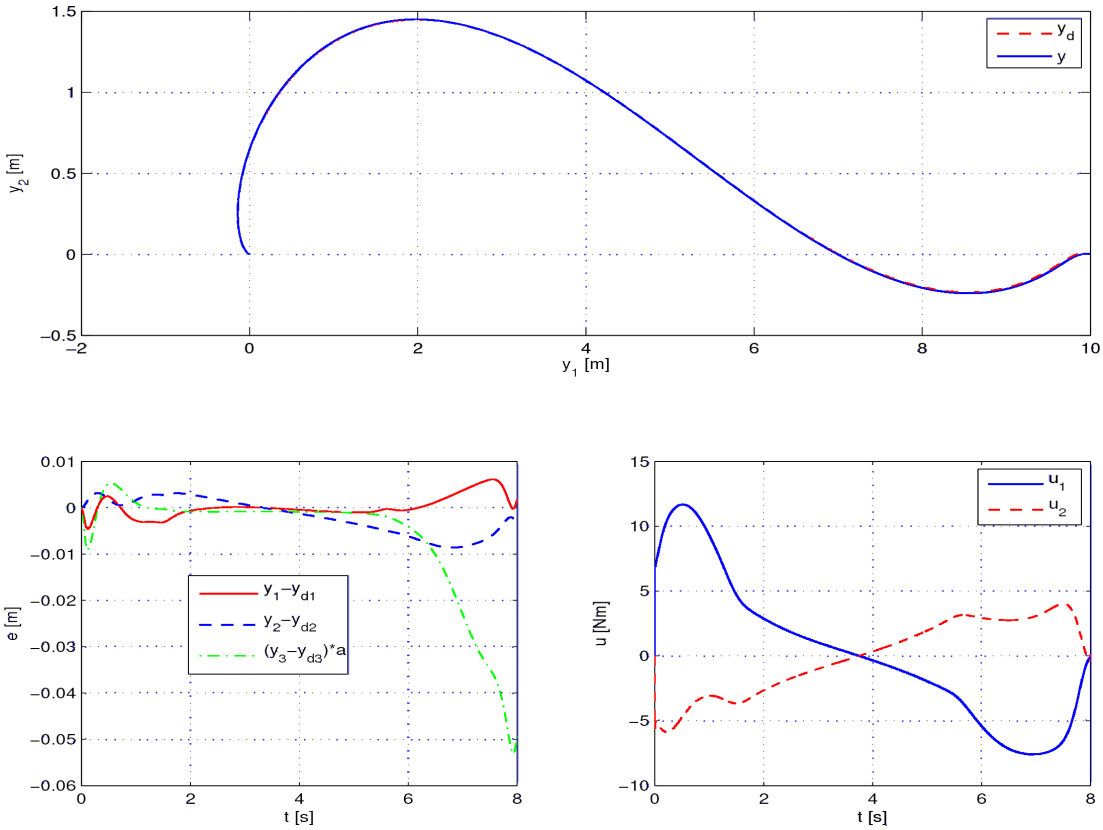

Fig. 5. Tracking, the nominal parameters: platform path, tracking errors, controls

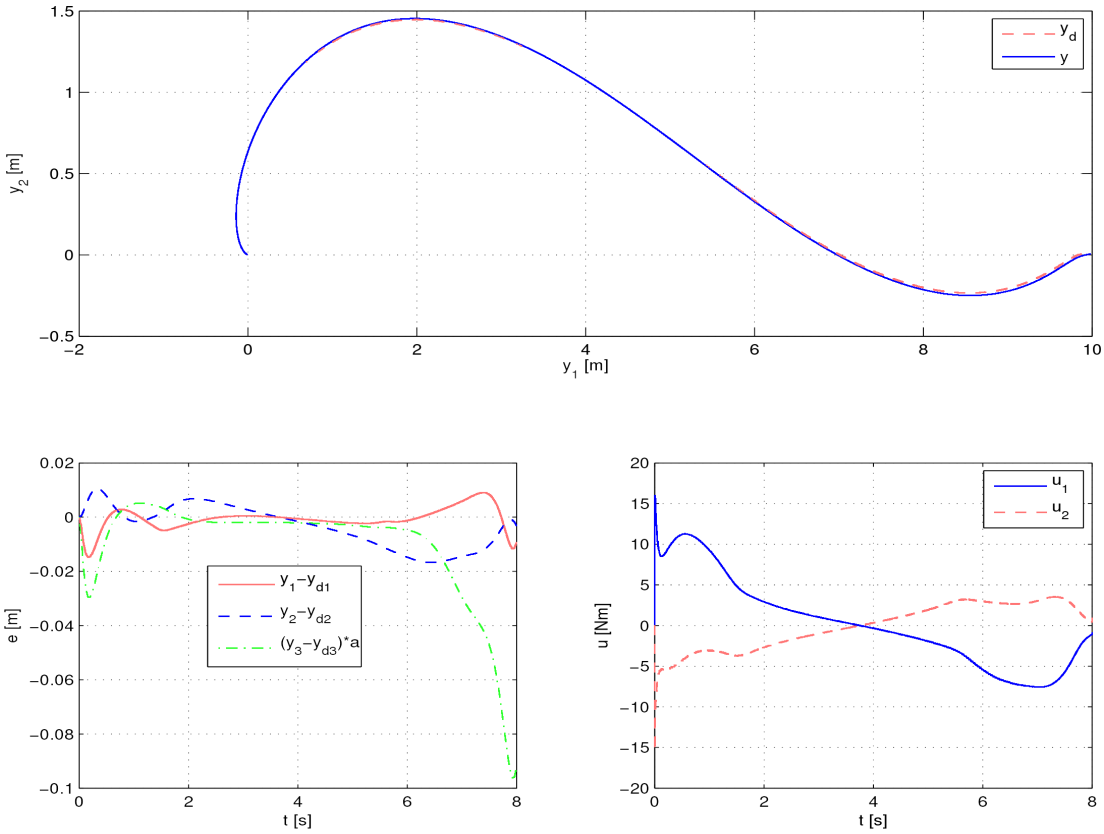

Fig. 6. Tracking, $Q_{13} = Q_{23} = 0$: platform path, tracking errors, controls

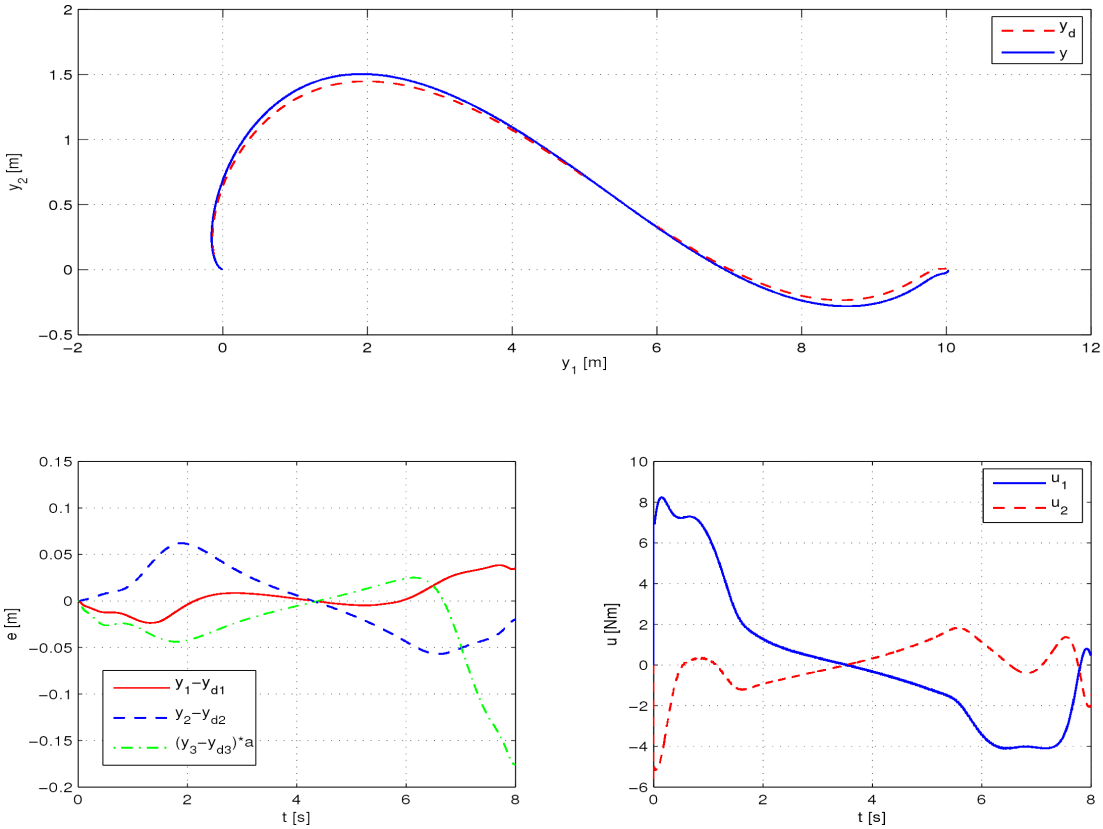

Fig. 7. Tracking, ϵ_i, τ_i decreased by 50 percent: platform path, tracking errors, controls

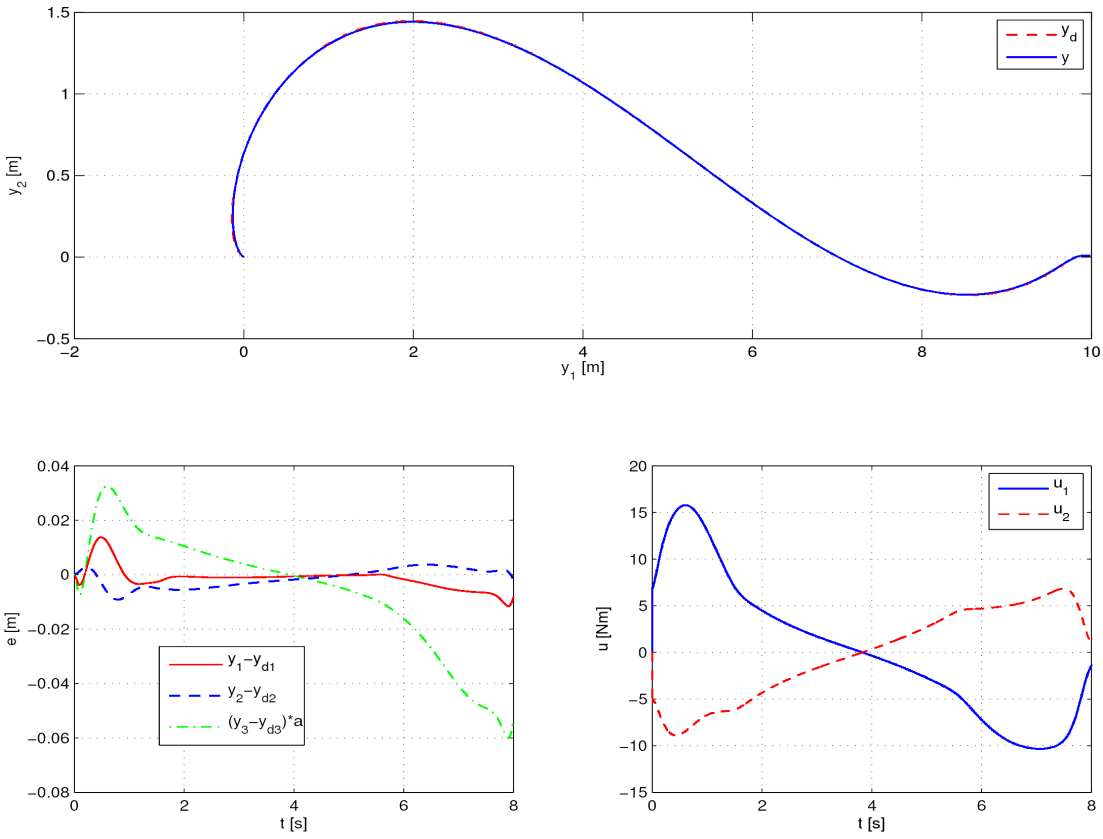

Fig. 8. Tracking, ϵ_i, τ_i increased by 50 percent: platform path, tracking errors, controls

6. Conclusions

We have studied modeling and control of the skid-steering Rex mobile platform. Depending on possible slip conditions of the wheels 16 variants of platform motion have been distinguished, dynamics equations for each variant provided. Special attention has been paid to the platform motion with all slips permitted. In this case the motion planning and the trajectory tracking problems have been addressed. Two motion planning algorithms have been proposed, one based on the Endogenous Configuration Space Approach, the other being an optimal control algorithm. In order to solve the tracking problem the Nonlinear Model Predictive Control has been used. Performance of these algorithms has been illustrated on an example of the parking problem. Remarkable robustness of the tracking algorithm has been demonstrated. In the computations of the optimal control as well the predictive control the ACADO software package has been exploited. A practically important advantage of ACADO is a possibility of generating a code that can be used as a tool for real time control of the Rex platform.

A part of this study devoted to the modeling of the Rex platform resulted in defining a switched control system with dynamic switching among 16 modes of operation. The motion planning and tracking control of such systems seems to be an open problem. Furthermore, the switching conditions, although well-defined theoretically, may appear difficult to detect in the real system. Taking this into account as well as for practical reasons we have concentrated on the motion with all slips of wheels allowed. These slips have been described directly as the velocities of the wheel's contact point with the ground, and the expression for the slip reaction forces is patterned on the recent proposals [13, 14], formally resembling the classical Burkhardt's formula [9]. A simplified, linear dependence of these forces on the slips is exploited. Correctness of this assumption needs to be verified experimentally, and if necessary, the full nonlinear model will be adopted. The motion planning and control algorithms of Rex are model-based. This means that when the design of Rex is completed, the final model parameters should be determined by means of an identification procedure. The tracking control of Rex is subordinated to the NMPC paradigm, whose robustness against incomplete knowledge of the model, and potential real time computability using ACADO tools has been confirmed in computer simulations. An experimental verification of this property, especially in connection with the state estimation of the Rex platform, is planned for the next future. These experiments will employ a dedicated the ROS-based programming framework that has already been implemented on Rex. Their results will be reported in a separate publication.

REFERENCES

[1] Y. Liu and G. Nejat, "Robotic urban search and rescue: a survey from the control perspective", *J. Intell. Robot. Syst.* 72, 147–165 (2013).

[2] K. Arent, M. Cholewiński, J. Malewicz, A. Mazur, J. Szrek, K. Tchoń, and K. Zadarnowska, "Conception of the mathematical and physical model of the experimental mobile platform Rex", *Report PRE* 9, CD-ROM (2013), (in Polish).

[3] C. Zieliński and T. Winiarski, "General specification of multi-robot control system structure", *Bull. Pol. Ac.: Tech.* 58, 16–28 (2010).

[4] K. Tchoń, K. Arent, M. Janiak, and Ł. Juszkiewicz, "Motion planning for the mobile platform Rex", in *Recent Advances in Automation, Robotics and Measuring Techniques*, pp. 497–506, Springer, Berlin, 2014.

[5] K. Kozłowski and D. Pazderski, "Modeling and control of a 4-wheel skid-steering mobile robot", *Int. J. Appl. Math. Comp. Sci.* 14, 477–496 (2004).

[6] M. Cholewiński, K. Arent, and A. Mazur, "Towards practical implementation of an artificial force method for control of the mobile platform Rex", in *Recent Advances in Automation, Robotics and Measuring Techniques*, pp. 353–363, Springer, Berlin, 2014.

[7] A. Mazur, "New approach to designing input-output decoupling controllers for mobile manipulators", *Bull. Pol. Ac.: Tech.* 53, 31–37 (2005).

[8] C.C. de Wit, B. Siciliano, and G. Bastin, *Theory of Robot Control*, Springer, New York, 1996.

[9] U. Kiencke and L. Nielsen, *Automotive Control Systems*, Springer, Berlin, 2000.

[10] H.B. Pacejka, *Tire and Vehicle Dynamics*, Elsevier, 2006.

[11] T. Kraus, H.J. Ferreau, E. Kayacan, H. Ramon, J. De Baerdemaeker, M. Diehl, and W. Saeys, "Moving horizon estimation and nonlinear model predictive control for autonomous agricultural vehicles", *Comp. Electr. in Agriculture* 98, 25–33 (2013).

[12] Z. Li and S.S. Ge, *Fundamentals in Modeling and Control of Mobile Manipulators*, CRC Press, Boca Raton, 2013.

[13] Ch.C. Ward and K. Iagnemna, "A dynamic-model-based wheel slip detector for mobile robots on outdoor terrain", *IEEE Trans. Robotics* 24, 821–831 (2008).

[14] K. Iagnemna and Ch.C. Ward, "Classification-based wheel slip detection and detector fusion for mobile robots on outdoor terrain", *Auton. Robot.* 26, 33–46 (2009).

[15] B. D'Andrea-Novel, G. Campion, and G. Bastin, "Control of wheeld mobile robots not satisfying ideal velocity constraints: A singular perturbation approach", *Int. J. Robust Nonlinear Control* 5, 243–267 (1995).

[16] T.M. Caldwell and T.D. Murphey, "Switching mode generation and optimal estimation with application to skid-steering", *Automatica* 47, 50–64 (2011).

[17] D. Liberzon, *Switching in Systems and Control*, Birkäuser, Boston, 2003.

[18] M. Opałka, "Motion planning of stratified systems", *Doctoral Dissertation*, Institute of Computer Engineering, Control and Robotics, Wrocław University of Technology, Wrocław, 2014.

[19] K. Tchoń and J. Jakubiak, "Endogenous configuration space approach to mobile manipulators: a derivation and performance assessment of Jacobian inverse kinematics algorithms", *Int. J. Control* 76, 1387–1419 (2003).

[20] A. Ratajczak and K. Tchoń, "Multiple-task motion planning of non-holonomic systems with dynamics", *Mechanical Sciences* 4, 153–166 (2013).

[21] J.B. Rawlings and D.Q. Mayne, *Model Predictive Control: Theory and Design*, Nob Hill Publishing, Madison, 2009.

[22] B. Houska, H.J. Ferreau, and M. Diehl, "ACADO Toolkit – an open-source framework for automatic control and dynamic optimization", *Optimal Control Methods and Application* 32, 298–312 (2011).

[23] M. Trojnacki, *Dynamics Modelling of Wheeled Mobile Robots*, PIAP Publishing House, Warsaw, 2013, (in Polish).

[24] K. Zadarnowska and K. Tchoń, "A control theory framework for performance evaluation of mobile manipulators", *Robotica* 25, 703–715 (2007).

[25] M. Janiak and K. Tchoń, "Constrained motion planning for nonholonomic systems", *Syst. Control Lett.* 60, 625–631 (2011).

[26] M. Diehl, H.G. Bock, H. Diedam, and P.-B. Wieber, "Fast direct multiple shooting algorithms for optimal robot control", in *Fast Motions in Biomechanics and Robotics*, ed. by M. Diehl and K. Mombaur, Springer-Verlag, Berlin, 2006.

[27] A. Mazur, M. Cholewiński, K. Arent, J. Malewicz, and J. Szrek, "Selected problems of modelling, control and design of a physical model of the search and rescue robot RobRex", *Report PRE* 9, CD-ROM (2013), (in Polish).